



Three-layered sandwich structured carbon film prepared by sputtering and ion/electron/ion alternative irradiation



Wenlei Zhang^{a,b}, Dongfeng Diao^{a,*}, Xue Fan^a

^a Institute of Nanosurface Science and Engineering (INSE), Shenzhen University, Shenzhen 518060, China

^b Key Laboratory of Education Ministry for Modern Design and Rotor-Bearing System, Xi'an Jiaotong University, Xi'an 710049, China

ARTICLE INFO

Article history:

Received 7 May 2015

Revised 30 July 2015

Accepted in revised form 1 August 2015

Available online 3 August 2015

Keywords:

Ion/electron/ion irradiation

Sandwich structure

Tribological properties

Mechanical properties

Carbon film

Electron cyclotron resonance (ECR) sputtering

ABSTRACT

The electron irradiated carbon film based on electron cyclotron resonance (ECR) sputtering technology has been proved to have both high conductivity and paramagnetism. However, the relatively low hardness, wear life and high surface roughness value limit its application in Micro-electromechanical Systems (MEMS). To improve these properties, the sandwich structured carbon films with different modulation ratios were introduced on silicon (100) wafers by alternative irradiation (ion/electron/ion) technique in ECR sputtering system. The three-layered nanostructure of films was measured with a transmission electron microscopy (TEM). The surface roughness of the film can be controlled to 0.19 nm according to the measurement of atomic force microscope (AFM). The unique characteristics of electron irradiated layer remained stable after irradiation through the analyzing of Raman spectroscopy. The mechanical properties (including hardness, elastic modulus, fracture behavior) and wear life were improved significantly due to the sandwich structure. The results showed that the sandwich structured carbon film is a kind of functional material equipped with enhanced mechanical and tribological properties.

© 2015 Elsevier B.V. All rights reserved.

1. Introduction

With the rapid development of nanotechnology, nano functional materials are required to have both good tribological and mechanical properties to cope with more complex application situations. Multilayer coating technique is one way to achieve the goal. Nano multilayer film is typically artificial materials composed of alternating layers with different materials. The thickness of each layer can be from several to hundreds of nanometers. The multilayer film system can overcome the disadvantages of monolithic film and has much better comprehensive properties [1–3]. Wang et al. prepared electron irradiated monolithic carbon film by electron cyclotron resonance (ECR) sputtering technique, which has been proved to have relatively high conductivity [4] and paramagnetism [5]. However, it was also found that this kind of film had the limitations of relatively low wear resistance, hardness and poor bonding strength with substrate, which means that it would suffer a higher risk in deformation, spalling and abrasion when facing a contact or friction in MEMS, leading to a change in conductive property [6] or magnetic degradation [7]. In order to improve the tribological and mechanical properties of the electron irradiated film, we constructed a three-layer

sandwich structured carbon film by using multilayer coating technique and assembling the electron irradiated film with relatively hard ion irradiated carbon film together. The ion irradiated layer lying between substrate and electron irradiated layer could serve as undercoat layer to enhance the bonding strength with the substrate.

Several studies about the properties of multilayer carbon films have been reported. Han et al. explored hardness, elastic modulus and stress trend of graded multilayer tetrahedral amorphous carbon film [8]. Xu et al. investigated the influence of modulation ratio on composition, hardness, residual stress, adhesion property and tribological characterization in four-layer carbon film [9]. Liu et al. developed a finite element model of multilayer carbon film with different layer number to analyze stress distributions induced by wear particles [10]. However, the multilayer carbon film in the aforementioned study was simply served as protecting films and seldom considered as functional materials. In this paper, we proposed an ECR ion/electron/ion alternating irradiation technique for fabricating a multilayer functional material, and a sandwich structured carbon film with hard/soft/hard layers was fabricated to evaluate the technique. The evaluating experiments using TEM, AFM and Raman spectra were carried out to analyze the structure, surface roughness and chemical composition respectively. The tests on hardness, elastic modulus, residual stress, fracture behavior and tribological characterization

* Corresponding author.

E-mail address: dfdiao@szu.edu.cn (D. Diao).

between monolithic and sandwich structured carbon film were also conducted to for exploring a novel functional material.

2. Experiment

2.1. Film preparation

The sandwich structured carbon films were deposited on Si (100) ($20 \times 20 \times 0.5$ mm) with ECR-sputtering technique [11]. Prior to the deposition, the chamber was pumped to a background pressure of 4.10×10^{-4} Pa and high purity argon was introduced into the chamber as the working gas with a pressure of 4.00×10^{-2} Pa. During the deposition, a DC bias voltage of -300 V was applied to the carbon target. The monolithic electron irradiated carbon film was fabricated at a substrate bias voltage of $+50$ V under the Mirror Confinement ECR (MCECR) mode [4]; while the ion irradiated film was deposited at a voltage of -5 V under the Divergent ECR (DECR) mode. All of the samples were prepared at room temperature. However, the substrate temperature of electron irradiated film raised up to 200 °C, while that of ion irradiated film almost remained the same during sputtering. The process of ECR ion/electron/ion irradiation is illustrated in Fig. 1. Five sandwich structured carbon films were obtained with different modulation ratios (deposition time ratio of an ion irradiated layer to an electron irradiated layer). The total deposition time for one film was 1500 s. Due to the different deposition rates between ion and electron irradiated layers and the possibility of ion etching, the total thickness of these films were not exactly the same. The detailed experimental parameters are shown in Table 1.

2.2. Characterization of films

The nanostructures of sandwich structured carbon films were observed using TEM (JEM-2100) with the electron acceleration voltage of 200 kV. TEM specimens for the cross-sectional view were prepared by mechanical polishing followed by argon-ion beam milling to a thickness appropriate for observation. The surface roughness measurement was carried out by using an AFM (Bruker Innova). The chemical composition was analyzed by Raman spectra (Horiba HR800) with a laser wavelength of 514 nm, and spectra region between 1100 and 3500 cm^{-1} . The conductivity was measured by the four-point probe method at room temperature.

The elastic modulus and hardness of the different structured carbon films were measured by a nanoindenter (Hysitron TI-900) and calculated by Oliver–Pharr method. In the test, a Berkovich diamond indenter with a tip radius of 200 nm and the maximum load of 1 mN were

Table 1

The experimental parameters of carbon films.

| Sample name | Deposition time of ion irradiated layer (bias = -5 V) | Deposition time of electron irradiated layer (bias = $+50$ V) | Modulation ratio (ion: electron irradiated layer) | Thickness |
|-------------|---|---|---|-----------|
| M0-E | – | 1500 s | – | 150 nm |
| M1 | 500 s | 500 s | 1:1 | 140 nm |
| M2 | 600 s | 300 s | 2:1 | 125 nm |
| M3 | 667 s | 167 s | 4:1 | 110 nm |
| M4 | 700 s | 100 s | 7:1 | 105 nm |
| M5 | 720 s | 60 s | 12:1 | 102 nm |
| M0-I | 1500 s | – | – | 100 nm |

used. A pre-test on quartz standard sample was done to calibrate the equipment. The value of the elastic modulus and hardness of the samples were given by averaging three different measurement results. The radius of curvature of the substrate was measured using a stylus profilometer (Ambios XP-2), and the residual stress was calculated through Stoney's formula [12].

$$\sigma_f = \frac{E_s d_s^2}{6(1-\nu_s) d_f} \left(\frac{1}{R_{post}} - \frac{1}{R_{pre}} \right)$$

where E_s , ν_s and d_s were the elastic modulus, Poisson's ratio and thickness of the Si (100) substrate, respectively. R_{pre} and R_{post} were the curvature radii of substrate before and after deposition. Fracture behavior was tested using the nanoindenter (Hysitron TI-900) as well. A cube diamond indenter with a tip radius of 50 nm and the maximum load of 10 mN were used to ensure the happening of fracture and compare with single amorphous carbon film [13]. The loading/unloading rate was 10 mN/min and holding time at maximum load was 5 s. The tribological experiments of the carbon films were operated on a ball-on-disk tribometer. The test conditions are at room temperature (23 °C) and a relative humidity about 40% . A Si_3N_4 ball was used for the frictional tests. The normal load was 1 N and sliding velocity was 19 mm/s with a frictional circle radius of 1.4 mm.

3. Experimental results and discussions

3.1. Nanostructures

Fig. 2 illustrates the cross-sectional view of two sandwich structured carbon films fabricated by ECR ion/electron/ion irradiation technique.

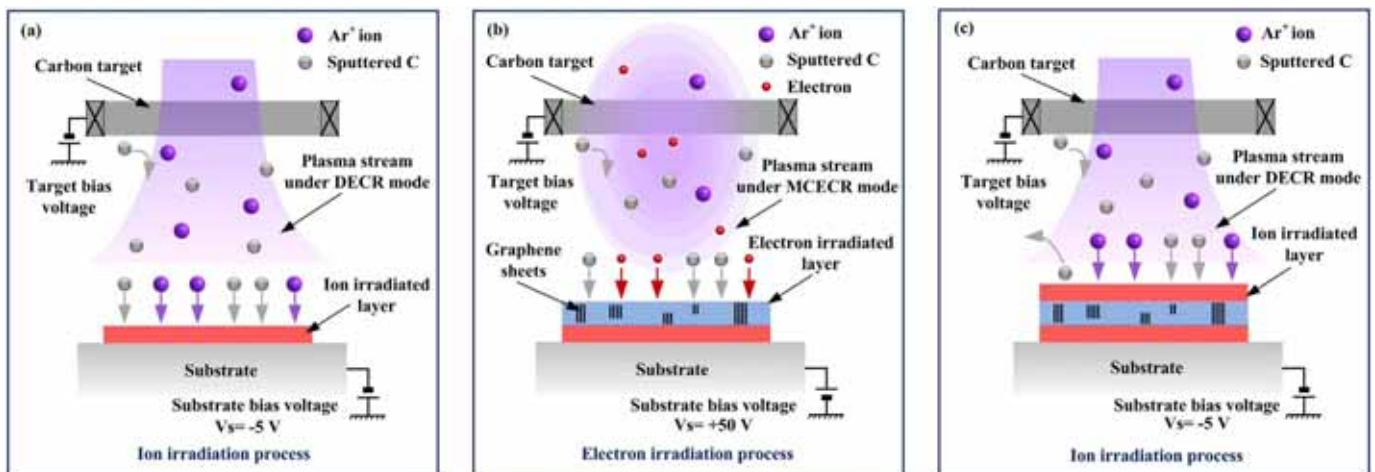


Fig. 1. Schematic illustration of the experimental design for ECR ion/electron/ion irradiation process. (a) Ion irradiation process of the first layer in sandwich structured carbon film. (b) Electron irradiation process of the second layer in sandwich structured carbon film. (c) Ion irradiation process of the third layer in sandwich structured carbon film.

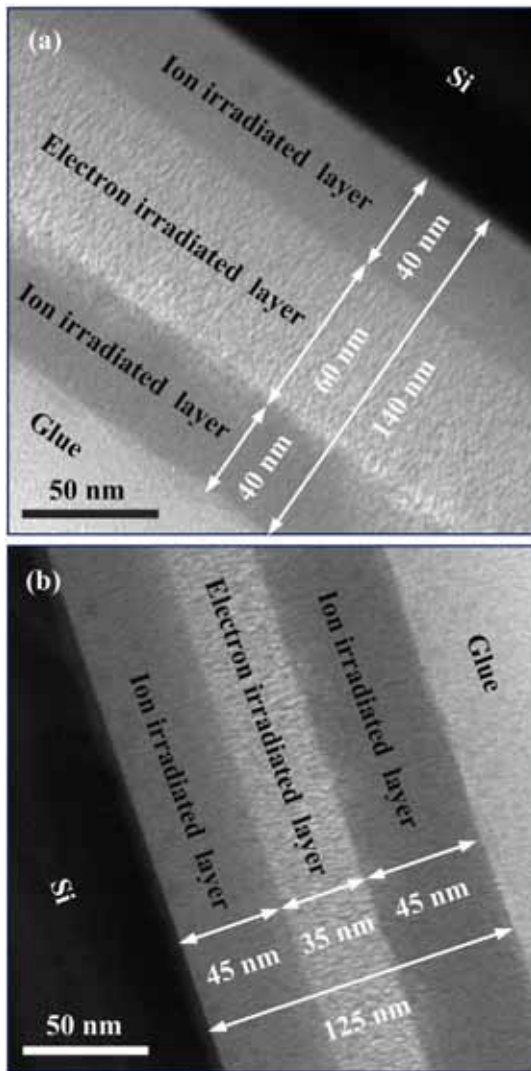


Fig. 2. Cross-sectional TEM images of sandwich structured carbon films (a) M1 and (b) M2.

The modulation ratios of the samples were 1:1 and 2:1, respectively. The TEM images confirmed a well-defined three-layered sandwich structure with one brighter layer wrapped by two darker ones. The first and the third darker layers were deposited by ion irradiation, while the brighter one in the middle was deposited by electron irradiation. The thicknesses of ion irradiated layer and electron irradiated layer in sample M1 were 40 nm and 60 nm, respectively. Since the deposition time of the three layers in sample M1 were same, it appears that the deposition rate of electron irradiated layer was higher than that of ion irradiated layer, which can also be confirmed by thicknesses of each layer in sample M2. The bright area outside the film was glue (M-Bond 610) and came from the preparation of TEM specimens.

The nanocrystalline structure with stacks of graphene sheets can be observed in the middle layer of sandwich structured carbon films, and the orientation of the graphene sheets was perpendicular to the substrate. The graphene sheets appeared when the irradiation energy was higher than 40 eV and may relate to the decline in electrical resistance according to Wang's work [4].

It should be noticed that the luminance between the ion irradiated layer and electron irradiated layer were totally different. One reason for this could be the density difference between two kinds of films. Future research could explore the relationship between luminance and density of different kinds of carbon films.

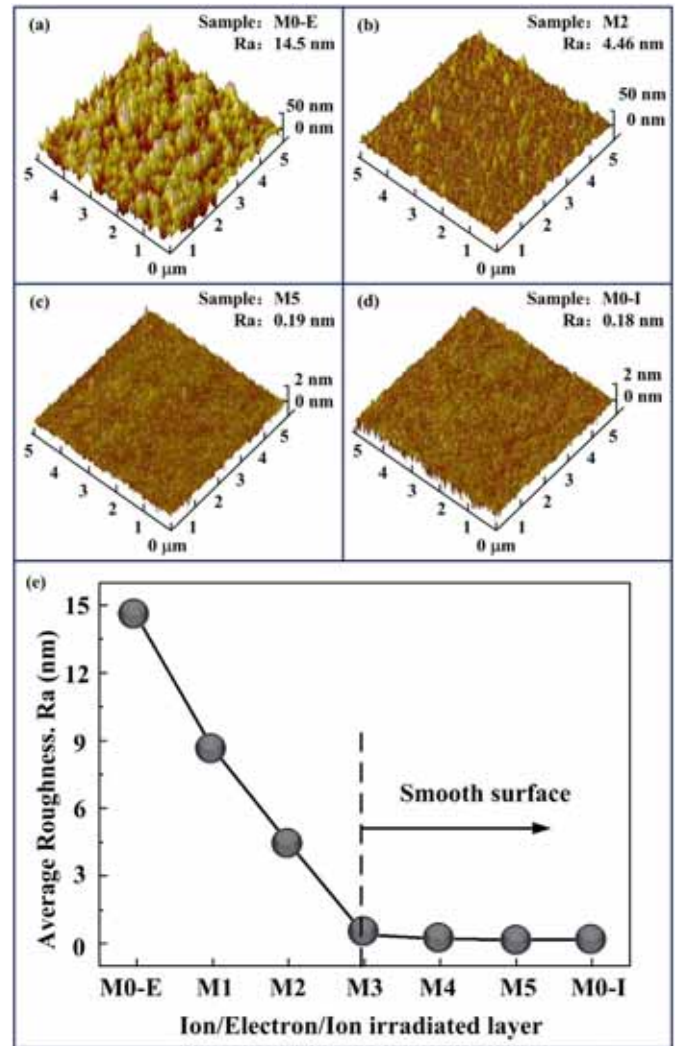


Fig. 3. Surface topographies of (a) electron irradiated film, sandwich structured carbon films (b) M2, (c) M5, (d) ion irradiated film, and (e) roughness of all samples.

3.2. Surface roughness

Fig. 3(a–d) shows the AFM images of monolithic carbon films and sandwich structured carbon films. The mean surface roughness (Ra) of electron irradiated film was relatively high (14.5 nm) due to the appearance of graphene sheets. With the sandwich structure, however, the roughness becomes smaller noticeably and decreased as the modulation ratio increased (Fig. 3(e)). A number of rough peaks can still be found in the AFM images of sample M2 (4.46 nm) with a low modulation ratio. However, the rough peaks disappeared when the modulation ratio was larger than 4:1 and the roughness was only around 0.2 nm (sample M3–M5), which was nearly the same as that of ion irradiated film (0.18 nm). This could be explained by the ion etching during the preparation of outermost ion irradiated layer. Since the deposition time of ion irradiated layer was longer in the case of sandwich structured carbon films with larger modulation ratio, the rough peaks would be etched effectively in these samples.

3.3. Chemical composition and conductivity

Fig. 4(a) depicts the Raman spectra of monolithic carbon films and sandwich structured carbon films with different modulation ratios fabricated on Si (100) substrate. The spectrum of ion irradiated monolithic

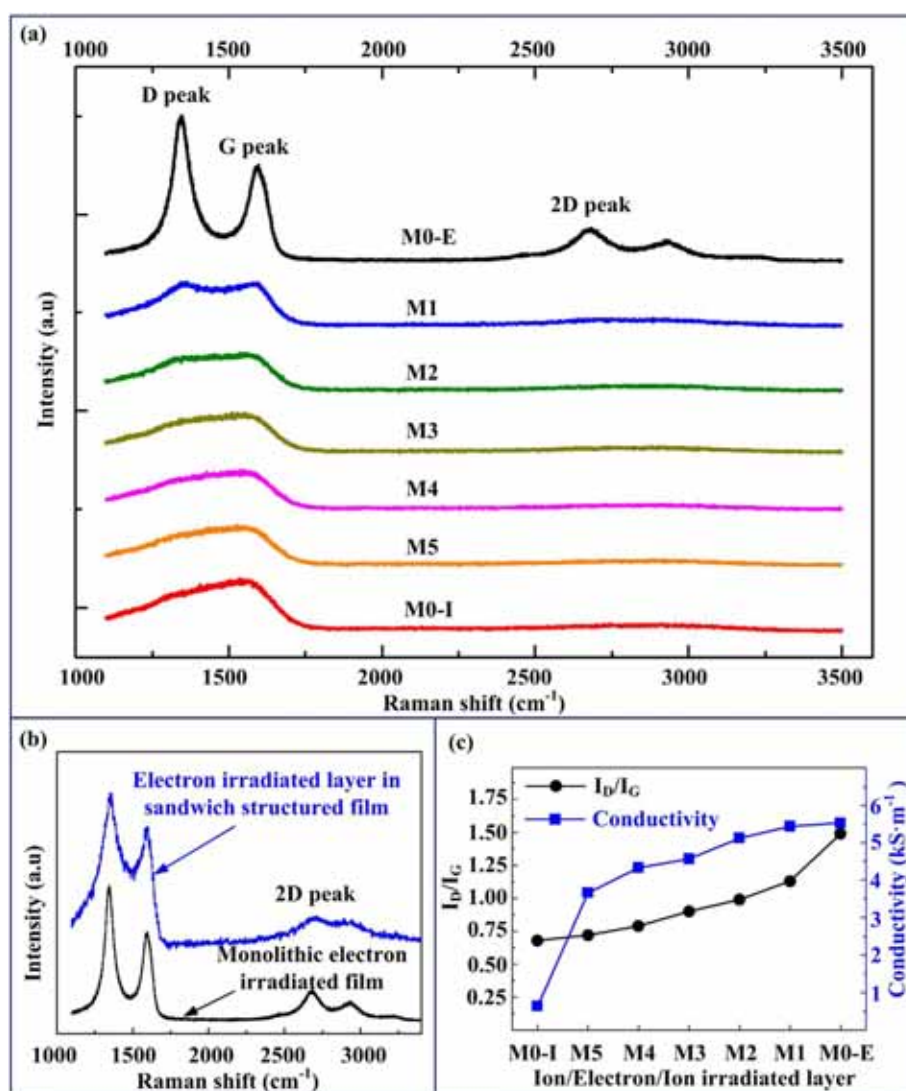


Fig. 4. (a) Raman spectra of the monolithic carbon films and sandwich structured carbon films. (b) Raman spectrum of electron irradiated layer in sandwich structure sample M1 fitting by difference Raman spectra. (c) Conductivity and I_D/I_G of the monolithic and sandwich structured carbon films.

carbon film exhibited a composite band centered around 1500 cm^{-1} . While the spectrum of electron irradiated monolithic carbon film showed separate D and G bands near 1340 cm^{-1} and 1600 cm^{-1} , and a 2D band, which was often observed in graphene or graphite samples [14], centered near 2700 cm^{-1} . The appearance of 2D band implies a structural transition from amorphous carbon to graphene sheets embedded carbon. These graphene sheets could lead to relatively high conductivity and paramagnetism of carbon films [4,5]. The spectra of sandwich structured carbon films changed gradually with increase of modulation ratios. The D and G bands still located separately in the sample M1 (modulation ratio of 1:1) but integrated in the sample M2–M5 as modulation ratio increased. The 2D band could hardly be seen in all of the sandwich structured carbon films.

The spectra region ranging from 1000 to 2000 cm^{-1} of all films was fitted by D and G peaks using Breit–Wigner–Fano (BWF) function to calculate the ratio of integrated intensities of D peak and G peak (I_D/I_G). As shown in Fig. 4(c), the I_D/I_G value of monolithic ion irradiated carbon film (sample M0-I) was the smallest among all samples, while the monolithic electron irradiated one (sample M0-E) was the largest. The I_D/I_G values of sandwich structured carbon film (sample M1–M5) lay between them, and increased with the decreasing of modulation ratio. Sheeja and Wei et al. had reported that the sp^2/sp^3 ratio was directly associated with the I_D/I_G . The greater I_D/I_G was, the larger sp^2/sp^3 ratio it

had [15,16]. Thus, it could be suggested that the sp^2/sp^3 ratio also increased with the decreasing of modulation ratio in the sandwiched structured films.

The spectrum of sandwich structured carbon film was analyzed to confirm whether the structure of electron irradiated layer in the film was changed during deposition. Since no 2D band was observed in sandwich structured carbon films, it is likely that the Raman signal of electron irradiated layer had been shielded under that of ion irradiated layers. A brief difference Raman spectra method [17,18] was used to separate the signal of electron irradiated layer from sandwich structured film. Fig. 4(b) shows the difference spectrum of electron irradiated layer in sample M1 and electron irradiated monolithic film (M0-E). The 2D band near 2700 cm^{-1} , separating D and G bands near 1340 cm^{-1} and 1600 cm^{-1} , which was a typical feature of electron irradiated film, was observed in the difference spectrum. These findings confirm that few changes happened to the electron irradiated layer during deposition and hence the layer still had its original properties. Fig. 4(c) presents the conductivity of all samples. The conductivity of electron irradiated monolithic carbon film and sandwich structured carbon films was six times greater than that of ion irradiated monolithic carbon film. However, the sp^2/sp^3 ratio of ion irradiated film and sandwich structured films did not exhibit such obvious gap according to the discussion above. It seems that the appearance of electron

irradiated layer led to the relatively low resistivity of sandwich structured films. An individual 2D peak was found in the difference spectrum of electron irradiated layer, inferring that the primary chemical composition of electron irradiated layer remains the same. While the measurement on conductivity further supported the inference that the properties of functional layer could preserve through the irradiation.

3.4. Mechanical properties

Fig. 5 shows the typical load–displacement curves of Si substrate, monolithic carbon films and sandwich structure film sample M2 with the maximum indentation load of 1 mN. Table 2 displays the hardness, elastic modulus and residual stress values of monolithic and sandwich structured films. The hardness and elastic modulus of electron irradiated monolithic carbon film were only 1.8 GPa and 45 GPa. The hardness and elastic modulus of sandwich structured films increased significantly with the values ranging from 3.3 GPa to 13.4 GPa and 109 GPa to 190 GPa, respectively. Since the maximum penetration depth of indenter went beyond the 20% of the film thickness, the value of hardness and elastic modulus were considered as a mixture of film and substrate [19]. The hardness and elastic modulus increased as modulation ratio increased, which were in agreement with the result of I_D/I_C . It is possible that the increase in the fraction of sp^3 bonded carbon atoms would enhance the hardness and elastic modulus of sandwich structured carbon films. Besides, the high residual stress in ion irradiated carbon is reduced by more than 50% through sandwich structure. Among all of sandwich structured films, sample M3–M5 with higher modulation ratio were most desired for the working situation with higher normal pressure due to their high hardness and elastic modulus.

The fracture behavior under higher load of monolithic carbon films and sandwich structured carbon films were analyzed from load–displacement curves. Fig. 6 illustrates the load–displacement curves of the monolithic and sandwich structured carbon films sample M2. In the load–displacement curve of sandwich structured carbon film, the first pop-in happened at the load of 3.5 mN. With the increase of indentation load, it began to show discontinuities which changed the slope of the loading curve at 3.5–6.5 mN. Another relatively small pop-in was found when the load reached 6.5 mN. Other sandwich structured films also exhibit such pop-in, discontinuities and pop-in pattern while only one pop-in was found in the curve of monolithic carbon films. One probable explanation may be attributed to the layer by layer fracture according to Li's study on monolithic carbon films [20]. The two pop-ins could be inferred as the fracture of two ion irradiated layers, while the discontinuities may be the spalling of electron irradiated layer.

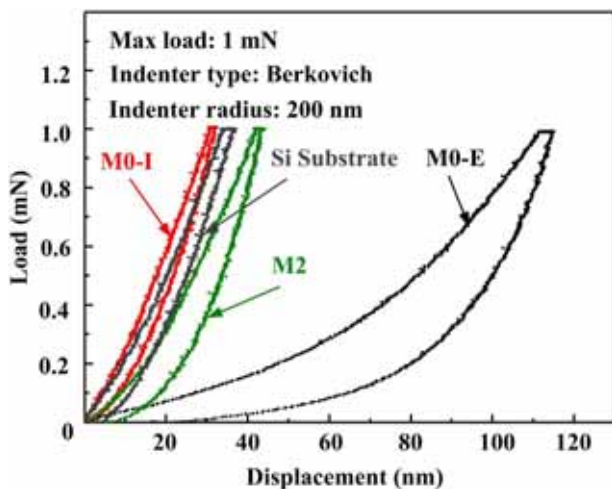


Fig. 5. The load–displacement curves Si substrate, monolithic carbon films and sandwich structured carbon films M2 with the maximum indentation load of 1 mN to obtain hardness and elastic modulus.

Table 2
Hardness, elastic modulus, residual stress, wear life and average friction coefficient of monolithic carbon films and sandwich structured films.

| Sample | Hardness (GPa) | Modulus (GPa) | Residual stress (GPa) | Wear life (Cycle) | Friction coefficient |
|--------|----------------|---------------|-----------------------|-------------------|----------------------|
| M0-E | 1.8 ± 0.2 | 45 ± 3 | −1.33 ± 0.07 | 45 ± 20 | 0.172 ± 0.038 |
| M1 | 3.3 ± 0.3 | 109 ± 5 | −5.26 ± 0.21 | 3140 ± 380 | 0.128 ± 0.027 |
| M2 | 8.6 ± 0.4 | 146 ± 8 | −5.27 ± 0.18 | 6100 ± 530 | 0.120 ± 0.023 |
| M3 | 9.6 ± 0.7 | 157 ± 16 | −6.82 ± 0.18 | 2520 ± 260 | 0.131 ± 0.029 |
| M4 | 11 ± 1 | 172 ± 15 | −7.93 ± 0.30 | 2400 ± 370 | 0.135 ± 0.030 |
| M5 | 13.4 ± 0.2 | 190 ± 3 | −8.23 ± 0.38 | 1610 ± 280 | 0.136 ± 0.030 |
| M0-I | 13.5 ± 0.3 | 191 ± 10 | −16.86 ± 0.69 | 1200 ± 340 | 0.163 ± 0.032 |

According to the discussion, the load for the second pop-in could be considered as the maximum load before the film spall completely. Since the load of second pop-in in sandwich structured films exceeded 6.5 mN, which was greater than that of the single pop-in in monolithic carbon films about 5 mN, it is concluded that the sandwich structure could bear higher load in the occasion of indentation and thus had better fracture behavior than the monolithic carbon films. This phenomenon agreed with Kot's work on Ti/TiN multilayer films and can be interpreted as the important role of electron irradiated layer on mechanical response, reducing the residual stress and increasing the fracture resistance [21].

The experiment results of mechanical properties indicate that the sandwich structured film equipped with relatively higher hardness, modulus and fracture resistance than those of electron irradiated film.

3.5. Tribological properties

Fig. 7 shows the typical tribological curves of friction coefficient for monolithic carbon films and sandwich structured carbon film M2. The electron irradiated monolithic carbon film had relatively weak tribological properties with the friction coefficient 0.172, and the value was about 0.4 after 45 cycles, which means the failure of film. The friction coefficient and wear life of ion irradiated monolithic carbon film were 0.163 and 1200 cycles individually. The friction coefficient of sandwich structure sample M2 was 0.140 at the beginning of tribotest, and decreased to 0.078 after about 4000 cycles. It could be due to the failure of the second electron irradiated layer, and then the graphene sheets lying inside lubricated the Si_3N_4 ball–carbon film friction pair. Table 2 also displays wear life and average friction coefficient of monolithic and sandwich structured films. The wear life of sample M2 was more than 6000 cycles, which was about 100 times longer than that of

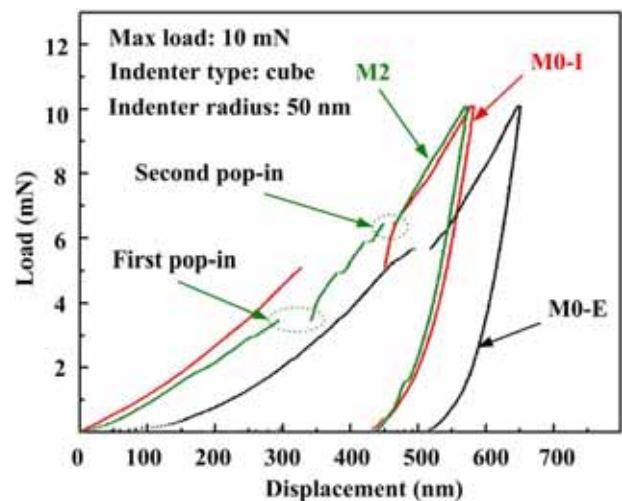


Fig. 6. The load–displacement curves of monolithic carbon films and sandwich structured carbon films M2 with the maximum load of 10 mN to obtain fracture behavior.

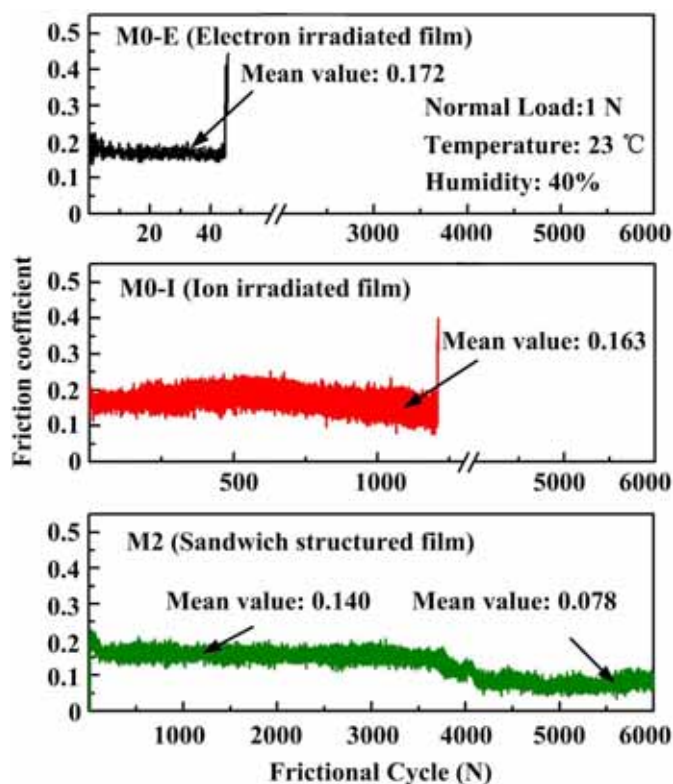


Fig. 7. The typical tribological curves of friction coefficient for electron irradiated monolithic carbon film, sandwich structured carbon film M2 and ion irradiated monolithic carbon film.

electron irradiated film and even 5 times more than that of ion irradiated film. Thus, sample M2 with the modulation ratio of 2:1 was most desired for the working situation with more abrasion. However, the average friction coefficients of all samples were approximate, ranging from 0.120 to 0.172.

These data reported here show an effective improvement on the wear life of electron irradiated film by adopting the sandwich structure, which shows a good agreement with the results of measurement on the hardness and surface roughness mentioned above. Moreover, the wear life of sandwich structured films is even longer than that of ion irradiated film. One reason for this could be that the electron irradiated layer acted as the internal stress relaxing layer [22] while the ion irradiated layers acted as the protective layer in the sandwich structured film, resulting in a good combination of internal stress and hardness in the sandwich structured films than that of monolithic films. Furthermore, the relatively high fracture resistance also produced a high wear life according to Ren and Kodali's study [23,24]. Our results suggest that the superior tribological properties of sandwich structure may be due to the improvement of mechanical properties [25,26].

4. Conclusions

In summary, an ion/electron/ion alternative irradiation technique was developed in electron cyclotron resonance (ECR) sputtering system for layered materials fabrication. By using this technique, a three-layered sandwich nanostructured carbon film was fabricated, where TEM image showing clearly that one electron irradiated layer was embedded between two ion irradiated layers. The mean surface roughness of the sandwich structured carbon film can be controlled at a relatively low value of 0.19 nm. The mechanical properties (hardness, elastic modulus, fracture behavior) and wear life were improved significantly

compared with electron irradiated monolithic carbon film. Among all sandwich structured samples, the ones with larger modulation ratio (M3–M5) had higher hardness and elastic modulus, while the ones with smaller modulation ratio (M1–M2) possessed longer wear life. In conclusion, the above results indicated that this technology can be expected for broad layered materials fabrication applications.

Acknowledgment

The authors thank the National Nature Science Foundation of China (Grant No. 91323303 and No. 51175405) and the Research Fund for the Doctoral Program of Higher Education of China (Grant No. 20120201110029).

References

- [1] J. Hong, J.Y. Han, H. Yoon, P. Joo, T. Lee, E. Seo, K. Char, B.S. Kim, Carbon-based layer-by-layer nanostructures: from films to hollow capsules, *Nanoscale* 3 (2011) 4515–4531.
- [2] S. Logothetidis, S. Kassavetis, C. Charitidis, Y. Panayiotatos, A. Laskarakis, Nanoindentation studies of multilayer amorphous carbon films, *Carbon* 42 (2011) 1133–1136.
- [3] C. Morant, S.G. Manyes, G. Sanz, J.M. Sanz, Elizalde, Nanotribological properties of CN/TiCN/TiN/Si multilayer as determined by AFM, *Nanotechnology* 16 (2005) 211–217.
- [4] C. Wang, D.F. Diao, X. Fan, C. Chen, Graphene sheets embedded carbon film prepared by electron irradiation in electron cyclotron resonance plasma, *Appl. Phys. Lett.* 100 (2012) 231909.
- [5] C. Wang, D.F. Diao, Magnetic behaviour of graphene sheets embedded carbon film originated from graphene nanocrystallite, *Appl. Phys. Lett.* 102 (2013) 052402.
- [6] S.R. Dupont, F. Novoa, E. Voroshazi, R.H. Dauskardt, Decohesion kinetics of PEDOT: PSS conducting polymer films, *Adv. Funct. Mater.* 24 (2014) 1325–1332.
- [7] S. Lee, M.Y. He, C.D. Yeo, G. Abo, Y.K. Hong, J.H. You, Effects of mechanical contact stress on magnetic properties of ferromagnetic film, *J. Appl. Phys.* 112 (2012) 084901.
- [8] X. Han, J.Q. Zhu, J.C. Han, M.L. Tan, Z.C. Jia, C.Z. Jiang, Stress, mechanical and adhesion properties of multilayer tetrahedral amorphous carbon films, *Appl. Surf. Sci.* 255 (2012) 607–609.
- [9] Z.Y. Xu, Y.J. Zheng, F. Jiang, Y.X. Leng, H. Sun, N. Huang, The microstructure and mechanical properties of multilayer diamond-like carbon films with different modulation ratios, *Appl. Surf. Sci.* 264 (2013) 207–212.
- [10] Y.J. Liu, X.L. Zhao, L.C. Zhang, D. Habibi, Z.H. Xie, Architectural design of diamond-like carbon coatings for long-lasting joint replacements, *Mater. Sci. Eng. C* 33 (2013) 2788–2794.
- [11] X. Fan, D.F. Diao, K. Wang, C. Wang, Multi-functional ECR plasma sputtering system for preparing amorphous carbon and Al–O–Si films, *Surf. Coat. Technol.* 206 (2011) 1963–1970.
- [12] J. Laconte, F. Iker, S. Jorez, N. Andre, J. Proost, T. Pardoen, D. Flandre, J.P. Raskin, Thin films stress extraction using micromachined structures and wafer curvature measurements, *Microelectron. Eng.* 76 (2004) 219–226.
- [13] X.D. Li, B. Bhushan, Measurement of fracture toughness of ultra-thin amorphous carbon films, *Thin Solid Films* 315 (1998) 214–221.
- [14] A.C. Ferrari, J.C. Meyer, V. Scardaci, C. Casiraghi, M. Lazzeri, F. Mauri, S. Piscanec, D. Jiang, K.S. Novoselov, S. Roth, A.K. Geim, Raman spectrum of graphene and graphene layers, *Phys. Rev. Lett.* 97 (2006) 187401.
- [15] D. Sheeja, B.K. Tay, S.P. Lau, X. Shi, X. Ding, Structural and tribological characterization of multilayer ta-C films prepared by filtered cathodic vacuum arc with substrate pulse biasing, *Surf. Coat. Technol.* 132 (2000) 228–232.
- [16] J. Robertson, Diamond-like amorphous carbon, *Mater. Sci. Eng.* 37 (2002) 129–281.
- [17] Z.C. Feng, B.S. Kwak, A. Erbil, L.A. Boatner, Difference Raman spectra of PbTiO₃ thin films grown by metalorganic chemical vapor deposition, *Appl. Phys. Lett.* 62 (1993) 349.
- [18] W. Kiefer, Raman difference spectroscopy with the rotating cell, *Appl. Spectrosc.* 27 (1973) 1572–1576.
- [19] B. Jonsson, S. Hogmark, Hardness measurements of thin films, *Thin Solid Films* 114 (1984) 257–269.
- [20] X.D. Li, D.F. Diao, B. Bhushan, Fracture mechanisms of thin amorphous carbon films in nanoindentation, *Acta Mater.* 45 (1997) 4453–4461.
- [21] M. Kot, Contact mechanics of coating-substrate systems: monolayer and multilayer coatings, *Arch. Civ. Mech. Eng.* 12 (2012) 464–470.
- [22] W. Zhang, A. Tanaka, B.S. Xua, Y. Koga, Study on the diamond-like carbon multilayer films for tribological application, *Diam. Relat. Mater.* 14 (2005) 1361–1367.
- [23] J. Ren, K. Kim, S.S. Kim, Fracture and tribological evaluation of dental composite resins containing pre-polymerized particle fillers, *J. Mater. Sci. Technol.* 19 (2003) 249–252.
- [24] P. Kodali, K.C. Walter, M. Nastasi, Investigation of mechanical and tribological properties of amorphous diamond-like carbon coatings, *Tribol. Int.* 30 (1997) 591–598.
- [25] J.H. Xu, H.B. Ju, L.H. Yu, Mechanical influence of silicon content on the microstructure, mechanical and tribological properties of magnetron sputtered Ti–Mo–Si–N films, *Vacuum* 110 (2014) 47–53.
- [26] M.A. Al-Bukhaitia, K.A. Al-hataba, W. Tillmannb, F. Hoffmannb, T. Sprute, Tribological and mechanical properties of Ti/TiAlN/TiAlCN nanoscale multilayer PVD coatings deposited on AISI H11 hot work tool steel, *Appl. Surf. Sci.* 318 (2014) 180–190.